



Hydrogeochemical characteristics and agricultural suitability of shallow groundwater quality in a concentrated coalfield area of Huaibei Plain, China

Yushan Tian · Quanli Liu · Yao Ji · Qiuling Dang ·
Yue Liu · Jing Su

Received: 22 November 2023 / Accepted: 8 August 2024
© The Author(s), under exclusive licence to Springer Nature Switzerland AG 2024

Abstract Groundwater is one of the chief water sources for agricultural activities in an aggregation of coal mines surrounded by agricultural areas in the Huaibei Plain. However, there have been few reports on whether mining-affected groundwater can be adopted for agricultural irrigation. We attempted to address this question through collecting 71 shallow groundwater samples from 12 coal mining locations. The Piper trilinear chart, the Gibbs diagram, the proportional coefficient of major ions, and principal component analysis were examined to characterize the source, origin, and

formation process of groundwater chemical composition. The suitability for agricultural irrigation was evaluated by a final zonation map that establishes a comprehensive weighting model based on analytic hierarchy process and criteria importance through the intercriteria correlation (AHP-CRITIC). The results revealed that the groundwater was classified as marginally alkaline water with a predominant cation of HCO_3^- and anion of Na^+ . Total hardness, total dissolved solids, sulfate (SO_4^{2-}), sodium (Na^+), and fluoride (F^-) were the primary ions that exceeded the standard. The results also indicated that the dominant hydrochemical facies were Ca- HCO_3 and Na-Cl. The dissolution of carbonate, silicate, sulfate minerals, along with cation exchange, were the main natural drivers controlling the hydrogeochemical process of groundwater. The zonation map suggested that 43.17%, 18.85%, and 37.98% of the study area were high, mediate, and low suitability zones, respectively. These results from this study can support policymakers for better managing groundwater associated with a concentration of underground coal mines.

Supplementary Information The online version contains supplementary material available at <https://doi.org/10.1007/s10661-024-12981-9>.

Y. Tian · Q. Liu · Y. Ji · Q. Dang · Y. Liu (✉) · J. Su (✉)
State Key Laboratory of Environmental Criteria and Risk Assessment, Chinese Research Academy of Environmental Sciences, Beijing 100012, China
e-mail: liu.yue@craes.org.cn

J. Su
e-mail: sujing@craes.org.cn

Y. Tian
e-mail: truoshan1998@163.com

Q. Liu
e-mail: liuql@craes.org.cn

Y. Ji
e-mail: byax0920@163.com

Q. Dang
e-mail: dangling819@126.com

Keywords Hydro-geochemistry · Groundwater quality · Coal mines · Agricultural suitability · Huaibei Plain

Introduction

The global demand for water resources has continued to significantly increase since the twenty-first century due to population increases, industrial development, and agricultural production activities. In arid regions where surface water is insufficient, groundwater is extensively utilized for irrigation and economic growth (de Graaf et al., 2019; P. Li et al., 2016; Saber et al., 2022). A vast majority of countries with major crops depend on partners who consume groundwater to produce crops (Dalin et al., 2017). The proportion of groundwater use in northern Chinese cities is as high as 66–72%, with 60% for industrial use and 45% for agricultural irrigation (Adimalla & Qian, 2019). However, the processes of extracting and utilizing groundwater carry out significant environmental consequences. Coal mining activities, a prevalent industry in many parts of China, produce a large amount of wastewater that is harmful if not well treated (Nordstrom et al., 2015). Several studies have shown that mine drainage is a source of recharge for shallow groundwater contamination, 20–30% of which is infiltrated into the shallow groundwater through irrigation (Keqiang et al., 2019). Tran et al. (2020) evaluated the potential repercussions of derelict coal mines on groundwater quality in the Ruhr coal field, Germany, and reported that SO_4^{2-} concentration was as high as 354 mg/L. Accordingly, coal mining activities threaten the sustainability and viability of water resources (Galhardi & Bonotto, 2016; P. Li et al., 2018). It is significant to understand the influence of human behavior on groundwater, such as coal mining activities (Wu et al., 2019). As such, this has a tremendous influence on human survival and health (Adimalla & Qian, 2021; Rodríguez-Lado et al., 2013; Sheng et al., 2022). It is therefore necessary to understand the hydrochemistry and water quality characteristics of groundwater in order to achieve effective management and sustainable development.

The dissolved components of groundwater mainly come from natural processes and anthropogenic sources, the natural sources mainly include water–rock action, weathering, mineral dissolution, etc. And anthropogenic sources have become the dominant contribution of dissolved components in groundwater (Sunkari et al., 2022). The increased knowledge of hydrogeochemical studies can help to identify these processes-controlled groundwater

hydrochemistry (Wu et al., 2015; Yang et al., 2016). Groundwater chemistry type and the relationships between major ions can effectively reveal water recharge sources and groundwater quality evolution in aquifers, and evaluate quality and suitability for usage for sound water management practiced (Srinivasamoorthy et al., 2012). Redwan et al. (2016) analyzed the impact of water–rock interaction mechanisms on groundwater quality using the Gibbs ratios. P. Li et al. (2016) applied the Durov diagram to confirm that mineral dissolution/precipitation and cation exchange are the primary natural factors controlling the hydrogeochemical formation of groundwater. This has also been carried out in similar research in Australia (Moya et al., 2015), China (He et al., 2021; Liu et al., 2021), Germany (Tessema et al., 2013), India (Khalid, 2019), Iran (Sajedi-Hosseini et al., 2018), and Pakistan (Adimalla & Qian, 2021), among others. Additionally, the multivariate statistical method (principal component analysis) reduces the workload by identifying the correlation within the variables, and at the same time, more accurately explains the main influencing factors (Qian et al., 2016; Wang et al., 2017). Consequently, integrating water chemistry techniques with principal component analysis enhances the comprehension of the pollutants' conditions and origins.

The great antidote to the assessment of groundwater quality and suitability for various demands about groundwater is conducting hydrochemical studies, irrigation water quality can be assessed by characterizing the ratio of various ion combinations (Subramani et al., 2005; Yang et al., 2016). Salinity and ion toxicity are the main problems in irrigation water. Sodium, as a conventional ion, is important in terms of concentration levels, and high sodium groundwater can react with soil, reducing permeability and leading to soil slumping, which directly affects crop yields (Zaman et al., 2018). Water with high TDS values is also viewed as unsuitable for drinking and irrigation (Fetter, 1990; Freeze & Cherry, 1979). It is obvious that irrigation water quality is significant for crop quality. Previous studies have identified several key indicators for evaluating irrigation water quality: Sodium Absorption Ratio (SAR), Sodium Percentage (Na%), Residual Sodium Carbonate (RSC), Permeability Index (PI), Magnesium Hazard (MH), Kelley's Ratio (KR), and Potential Salinity (PS), Wilcox, and US Salinity Laboratory (USSL) classifications, etc.

(Bauder et al., 2011; Bortolini et al., 2018; Chemura et al., 2014; Dhaouadi et al., 2022). However, while the single factor index method is straightforward to apply, it falls short in providing a holistic assessment of individual indicators, making it challenging to fully characterize water quality. Therefore, it necessitates the depiction of the irrigation water quality status through an efficient conversion into a Water Quality Index (WQI) score, utilizing a range of environmental parameters (Chowdhury et al., 2022; Wu et al., 2021). Among them, comprehensive evaluation method emphasizes determining the weights of the assessment indicators. The analytic hierarchy process (AHP) is a broadly applied method for addressing multi-objective dilemmas, allowing for the weighting of evaluation criteria based on their influence on the quality of irrigation water (Elvis et al., 2022; Zhong et al., 2022). Rajkumar et al. (2022) discovered that the Comprehensive Water Quality Index (CWQI), developed utilizing the AHP method, demonstrated its effectiveness as a robust and thorough method for assessing groundwater quality, outperforming both WQI and IWQI. However, AHP method carries inherent subjectivity in manual weight assignment. The criteria importance through the intercriteria correlation (CRITIC) method adeptly capitalizes on the inherent objectivity of data to ascertain the indicator weights in multi-indicator dilemmas (Zhang et al., 2021). A combination of AHP and CRITIC methods amplifies their individual strengths, leading to a more accurate and dependable assessment of multi-indicator problems (Li et al., 2021; Xiao et al., 2023).

The study area has many coal mines, and groundwater is often extracted for irrigation in agricultural production activities due to low drilling costs and easy availability. Currently, many agricultural irrigation areas exist around the mines. However, existing studies have only assessed groundwater quality standards. Meanwhile, the availability of nearby groundwater resources for agriculture activities is unknown. As such, it is imperative to determine whether groundwater in such mining areas can be used for irrigation. The primary objectives of this paper were to (1) ascertain the hydrogeochemical properties of groundwater and water chemistry facies, evaluating spatial variations of water chemical parameters; (2) understand the groundwater water-rock interaction and mineralization processes, elaborate ion sources, and determine the controlling mechanisms of water

chemistry in the area; and (3) evaluate the groundwater quality in agricultural irrigation areas establishing a comprehensive weighting model based on AHP-CRITIC and determine suitability. The findings will help in formulating irrigation management strategies for developing rational use of groundwater in mining areas, which is significant for maintaining the security of the local agroecological environment.

Materials and methods

Study area

There are roughly 2741 km² in the research area located in the Huaibei Plain. The terrain type is relatively simple and slopes from northwest to southeast. The landform is dominated by plains, with low mountains and hills, mountain stream basins, and flood alluvial plains. The region is located in the middle latitudes and pertains to the warm temperate semi-humid monsoon climate zone distinguished by obvious monsoon, distinct seasons, mild climate, and moderate rain. The annual mean temperature is 14.8 °C, with July recording the highest temperature (40.4 °C) and January recording the chilliest (3.1 °C). The annual mean evaporation and drought index is 918.0 mm and 1.1, respectively. The mean annual rainfall is 849.6 mm and is accumulated from June to September. Precipitation forms a slope runoff, which gathers into ditches, rivers or artificial village ponds, subsidence depressions, and forms surface water. Due to a reduction of precipitation in drought years, river runoff is greatly reduced, which reflects that the rivers in the area are all rain-sourced rivers, and their resources are completely dependent on the amount of precipitation replenishment. The important economic source in this region is coal mining and agriculture, with coal revenues accounted for 43.9% of total revenues, cropland area covering 1675.11 km², accounting for 96.7% of the total land area, while surrounded the coal mining areas are mostly agricultural irrigation areas.

Geology and hydrogeology

The eastern and western parts of the region are covered by large Quaternary loose layers, as well some Cambrian and Ordovician carbonate rocks are

exposed in the north, which the overall flow direction is from northwest to southeast. Based on the lithology, occurrence characteristics, hydraulic connection, the Quaternary loose sand aquifer from the top

down contains the first aquifer (the main sampling aquifer), the second aquifer, the third aquifer, and the fourth aquifer (Fig. 1c) (Qiu et al., 2023). The first aquifer used for agricultural irrigation and rural

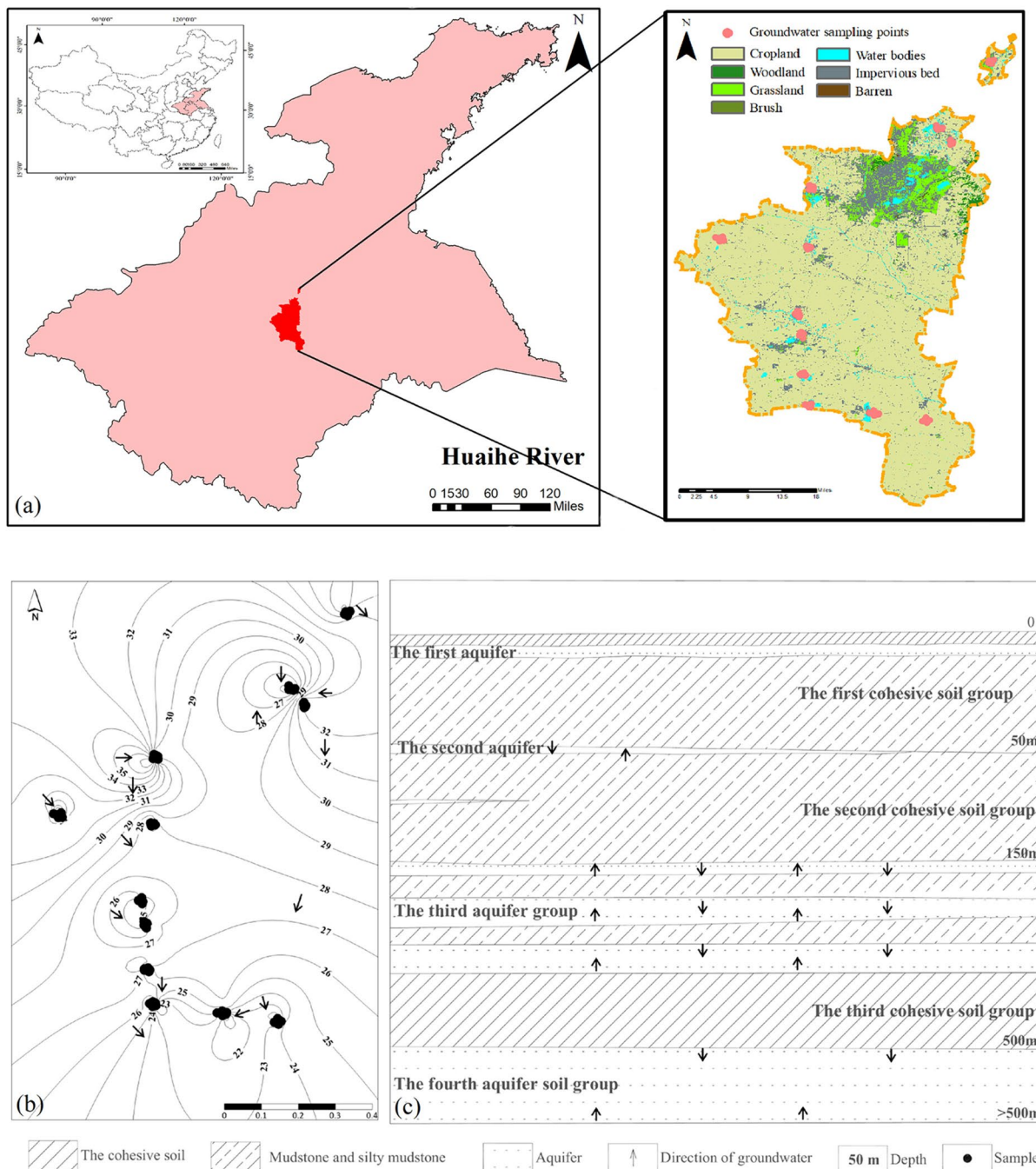


Fig. 1 a Location of the study area and sampling wells, b depth to water level map, and c diagram of aquifer structure in the research area

drinking water is regarded as a shallow aquifer, which has been polluted to varying degrees due to industrial activities such as regional coal mining in recent years, and the second, third, and fourth aquifers with deep burial are currently of good quality; thus, this investigation focuses on shallow groundwater as the object of study. The shallow aquifers are dominated by fine sandy clay, and the hydraulic property are phreatic groundwater. The main recharge mode is precipitation infiltration, followed by infiltration from rivers and water storage projects during flood season, irrigation re-infiltration and upstream (outside the area) underground runoff water, etc. The discharge is mainly by vertical evaporation.

Sample collection and analysis

The monitoring sampling includes 12 coal mines and each coal mine had several control monitoring points, located in the mine impact area upstream boundary 30–50 m, at three pollution dispersion monitoring points, groundwater downstream and within 50 m on both sides, one or two internal mine monitoring points, respectively, located in the temporary gangue pile and sewage disposal station within 30 m downstream.

In November 2021, 71 groundwater samples were collected throughout the investigation region, pumped and sampled from new monitoring wells in the coal mine and from surrounding residential wells (Fig. 1a). Wells were washed prior to sampling, and after completion of sampling, the containers were pre-cleaned 500 mL polyethylene or glass bottles, labeled for sampling, and preserved at 4 °C until laboratory test. The whole samples are collected, stored, and examined in compliance with national technical standards (China, HJ164–2020). Surveyed parameters included pH, total hardness (TH), total dissolved solids (TDS), redox potential, electrical conductivity (EC), permanganate index, dissolved oxygen (DO), major ions (Na⁺, K⁺, Ca²⁺, Mg²⁺, SO₄²⁻, HCO₃⁻ Cl⁻), nitrate (NO₃-N), nitrite (NO₂-N), ammonia nitrogen (NH₄-N), fluoride (F⁻), and trace metals (Fe, Mn, Cu, Zn, Hg, As, Sn, Cd). A portable multi-parameter analyzer was adopted to measure pH, redox potential, EC, and DO in situ. The EDTA titrimetric method was adopted to measure Ca²⁺ and Mg²⁺. The measurement of major cations and trace metals were determined by inductively coupled plasma mass spectrometry (ICP-MS) with

a precision of 1%. Cl⁻, NO₃-N, SO₄²⁻ were analyzed by ion chromatography (Rowell, 2014). The concentration of F⁻ was determined through an ion selective electrode method. The UV spectrophotometric method was used to measure the concentrations of NO₂-N and NH₄-N (Zhai et al., 2022).

Statistical analysis

Spearman correlation coefficients

Correlation analysis reflects the level of relationship between different ions in groundwater, and since the concentration data were processed as continuous variables, while did not follow to be normally distributed, the Spearman correlation coefficient was adopted to characterize the distribution.

Spearman’s correlation coefficient is commonly denoted by the Greek letter ρ to indicate its value to evaluate the relationship between two ranks (Schroeder et al., 2010). The basic idea is Spearman’s correlation coefficient utilizes the data rank of each variable instead of the raw data, ranks raw data from low to high, then the difference between the rankings is used as the main input to the following equation.

$$\rho_s = 1 - \frac{6 \sum_{i=1}^n (U_i - V_i)^2}{n(n^2 - 1)} = 1 - \frac{6 \sum_{i=1}^n D_i^2}{n(n^2 - 1)} \quad (1)$$

U_i and V_i are ranks of two variables.

When coefficient ρ_s is 0, the two variables are completely independent, ρ_s equals +1 if the two variables are completely in same concordance, otherwise, -1 if the two variables are completely reversed.

Principal component analysis (PCA)

Combining the results acquired from Spearman’s correlation interpretation, the following indicators (total hardness, total dissolved solids, sulfate, chloride, sodium, calcium, magnesium, conductivity, and fluoride) were selected to extract the main influencing factors of groundwater quality by PCA. PCA is a dimensionality reduction method, by studying the internal correlation between the main indicators in the sample, exploring the basic structure in the data, and combining the original variables in different proportions by weighted averaging to generate new

variables, which can cover almost all information (Menció et al., 2012; Moore et al., 2009).

Agricultural suitability assessment

Abundant shallow groundwater in the region is an essential resource for agricultural activities. Shallow groundwater is the predominant layer in agricultural fields; thus, ascertaining water quality is fundamental significance for assessing the quality and yield of crops. The following metrics were used to analyze the groundwater (Na%, SAR, RSC, MH, KR) to evaluate irrigation groundwater quality (Bauder et al., 2011).

$$Na\% = \frac{(Na^+ + K^+) \times 100}{Ca^{2+} + Mg^{2+} + Na^+ + K^+} \quad (2)$$

$$SAR = \frac{Na^+}{\sqrt{(Ca^{2+} + Mg^{2+})/2}} \quad (3)$$

$$RSC = (CO_3^{2-} + HCO_3^-) - (Ca^{2+} + Mg^{2+}) \quad (4)$$

$$MH = \frac{Mg^{2+}}{Ca^{2+} + Mg^{2+}} \times 100 \quad (5)$$

$$KR = \frac{Na^+}{Ca^{2+} + Mg^{2+}} \quad (6)$$

Comprehensive evaluation model

In order to enable a comprehensive evaluation of the irrigation index in the study area, AHP-CRITIC (combining the subjective assignment method with the objective assignment method) was utilized to determine the weights of multiple indicators (Y. Li et al., 2021), which steps are described in the following:

Step 1: Evaluation indicator identification: irrigation index evaluation indicators include EC, SAR, Na%, Cl^- , MH, RSC, KR, TH, pH.

Step 2: Subjective weighting calculation (B_j): AHP was used to investigate the suitability of irrigation, and different weights (Table S1) were assigned to these parameters using the two relative comparison matrices of AHP according to the degree of influ-

ence of irrigation suitability parameters on water quality (Abdelkarim et al., 2023).

Step 3: Dimensionless processing of indicators:

$$\text{Negative indicators : } y_{ij} = \frac{x_{ij} - x_{j,\min}}{x_{j,\max} - x_{j,\min}} \quad (7)$$

$$\text{Positive indicators : } y_{ij} = \frac{x_{j,\max} - x_{ij}}{x_{j,\max} - x_{j,\min}} \quad (8)$$

$$\text{pH : } y_{ij} = \frac{x_{i,j} - \bar{x}_{ij}}{x_{j,\max} - x_{j,\min}} \quad (9)$$

x_{ij} denotes the value of j th evaluation indexes of i th mixing procedures.

Step 4: Calculation of standard deviation and conflict (correlation coefficients): where m and n represent the values of mixing procedures and evaluation indexes, and $r_{jj'}$ denotes the correlation coefficient between the indexes j' and j .

$$S_j = \sqrt{\frac{\sum_{i=1}^m (y_{ij} - \bar{y}_j)^2}{m-1}} \quad (10)$$

$$\bar{y}_j = \frac{1}{m} \sum_{i=1}^m y_{ij} \quad (11)$$

$$R_j = \sum_{j'=1}^n 1 - r_{jj'} \quad (12)$$

Step 5: Determination of objective weight and comprehensive weight:

$$C_j = \frac{S_j R_j}{\sum_{j=1}^n S_j R_j} \quad (13)$$

$$W_j = \frac{B_j C_j}{\sum_{j=1}^n B_j C_j} \quad (14)$$

Data processing

Statistical analysis methods were adopted to process the data, and principal component analysis was applied to estimate the elements that may affect

hydrochemistry. Piper plot, Gibbs plot, and ion ratio methods were adopted to elaborate on water chemistry. The water chemistry data statistics and correlation analysis were completed using Origin 2022b software. The formation of spatial distribution maps was shown by the inverse distance weighted (IDW) interpolation technique in ArcGIS software.

Results

Ion content statistics of groundwater

Table S2 displays the hydrochemical parameter analyses for groundwater, which present the minimum, maximum, 25th percentile, median, 75th percentile, average, standard deviation, coefficient of variation, III water standard, and non-detect rate.

In the present investigation, the pH value of groundwater was neutral, varying from 6.7 to 8, the total hardness ranges between 77.2 and 1550 mg/L, and exceedance rate (groundwater class III water standard) was 40.85%, which may lead to heart disease and kidney stones (Sengupta, 2013). The redox potential varied from 34.6 to 354, which is a reducing environment. EC value varies from 2.11 to 1782 $\mu\text{S}/\text{cm}$, and the EC value is affected by the ionic composition and salinity of the groundwater (Hubert & Wolkersdorfer, 2015; Subramani et al., 2005; Yadav et al., 2011). The variation range of TDS concentration was 0.3–3.0 g/L. In accordance with TDS concentration, Freeze and Cherry (1979) classified water as freshwater (TDS < 1000 mg/L), brackish water (> 1000 mg/L), saline water (> 10,000 mg/L), and brine (< 100,000 mg/L). In our research area, 43.66% of the groundwater was brackish. The permanganate index can accurately reflect the content of organic and inorganic matter in water, with values varying between 0.43 and 5.22. The DO value ranged from 1 to 8.4 mg/L.

For the eight major ions in water, in general, the main anion concentration shows $\text{HCO}_3^- > \text{SO}_4^{2-} > \text{Cl}^-$. The concentration of main cation is $\text{Na} > \text{Ca} > \text{Mg} > \text{K}$. The dominant ions are HCO_3^- and Na, comprising 89.75–22.97% of the total number of all anions and cations, respectively. There are some points where SO_4^{2-} , Cl^- , and Na exceeded the standard, and the exceedance times were 40.85%, 28.17%, and 46.48%, respectively. Fluoride

concentrations ranged from 0.53 to 3.47 mg/L; meanwhile, approximately 64.79% of the points outweigh the allowable limit (1.0 mg/L) and may cause fluorosis (Siddique et al., 2022).

Among the nutrient salt indicators, nitrate, as a natural ion, about 5.6% of the sites exceed the limit value of 20 mg/L, and 47 sites severely exceeded concentration levels that could lead to health hazards (Peterson et al., 2001; Y. Zhang et al., 2018). The concentration variation of nitrite in the region ranged from 0.001 to 0.516 mg/L, which do not exceed the standard limit. Ammonia nitrogen varied from 0.26 to 1.54 mg/L, and seven points exceeded the standard restriction.

Among the trace element indicators, iron and manganese concentrations varied from 0.01 to 6.36 mg/L and 0.006 to 2.11 mg/L, respectively, with 19.72% and 70.42% of sample points exceeded the standard limits, probably due to the high concentration of environmental background values in the region. The heavy metal indicators, except for lead, were negligible and within the acceptable limits. The range of lead variation values was 0.00009–0.154 mg/L, with the maximum value occurring at point 64.

The coefficients of variation for sulfate, potassium, ammonia nitrogen, nitrite, nitrate, iron, manganese, zinc, selenium, cadmium, and lead exceeded 100%, indicating that they showed a large variation at all points.

Spatial variability of groundwater hydrochemistry

Inverse distance weighting (IDW) is an accurate interpolation method, which can ensure that the interpolation result sampling points are the same as the actual monitoring value. Also, IDW is able to handle data outliers, and compared to other interpolation methods, it is easier to determine unknown region results (Gidey, 2018; Haldar et al., 2020). In accordance with the hydrochemical indicators of groundwater as described above, the spatial distribution maps were plotted with ArcGIS software 10.4 as demonstrated in Fig. 2. The greatest TDS concentration was principally in the northwest area, with an increasing trend from south to north, especially at points 3, 7–14, and 48–53. TDS values were larger, and the maximum value occurs at point 50, with large spatial variability, probably due to geochemical processes and coal mining in the area (A. K. Tiwari et al., 2016). The content

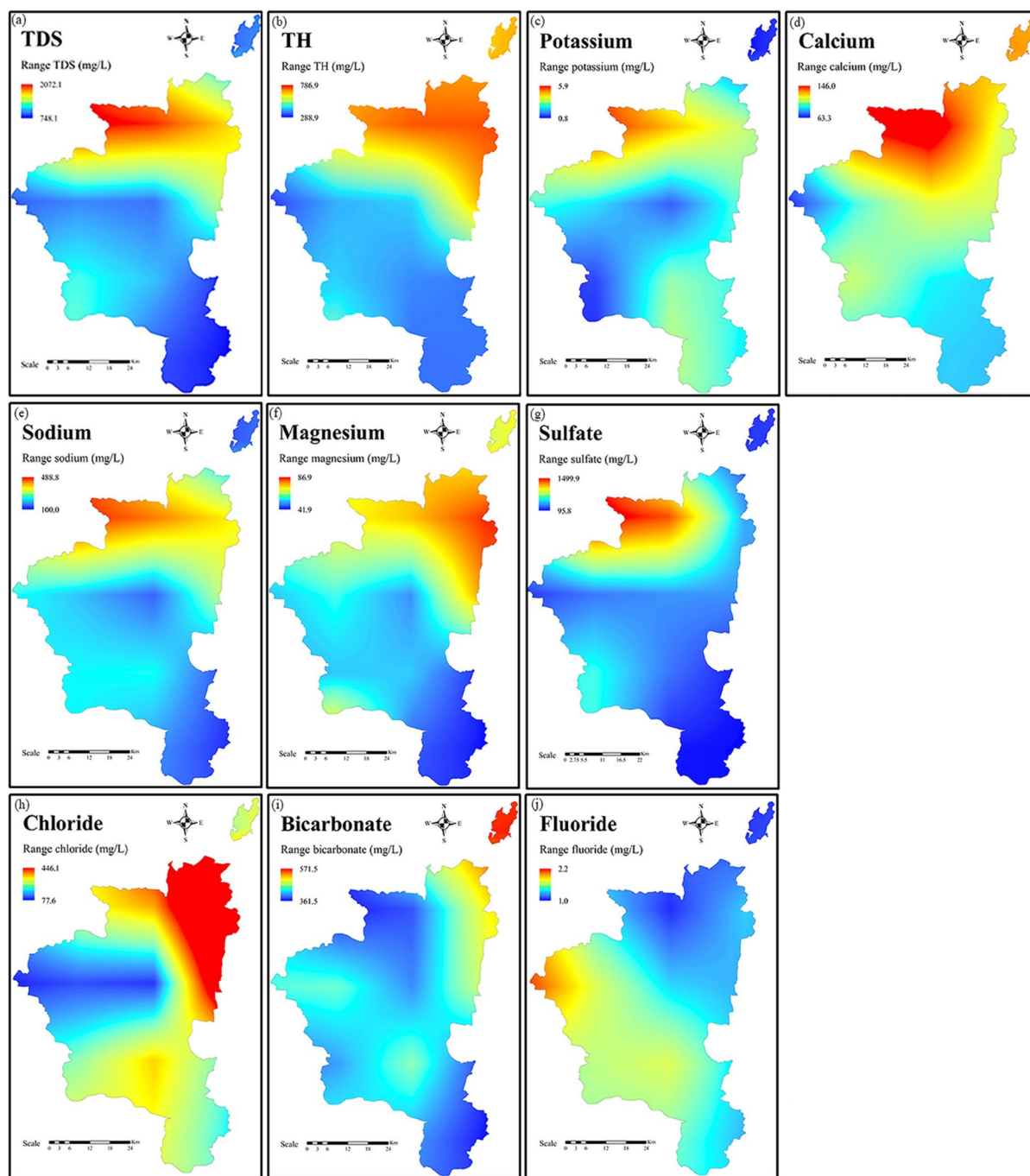


Fig. 2 Spatial distribution maps of hydrochemical parameters of groundwater: **a** total dissolved solids (TDS), **b** total hardness (TH), **c** potassium (K^+), **d** calcium (Ca^{2+}), **e** sodium

(Na^+), **f** magnesium (Mg^{2+}), **g** sulfate (SO_4^{2-}), **h** chloride (Cl^-), **i** bicarbonate (HCO_3^-), **j** fluoride (F^-)

of K^+ was low compared with other ions, and its spatial distribution was consistent with TDS, Ca^{2+} and Na^+ . Na^+ might be connected to the cation exchange

mechanism, whilst calcium and magnesium ion might derive from the leaching of calcium- and magnesium-containing rocks in the region. SO_4^{2-} in groundwater

mainly comes from dissolution and precipitation in rocks containing sulfur compounds, and the high concentration points appeared at points 49–53, representing the northeast red area. Cl^- was distributed in the same way as Mg^{2+} , with higher concentrations in the northeast region. The distribution of F^- was different from that of other substances, and the peak area appeared in the western region. F^- concentrations in the study area are essentially attributed to geological factors (Saxena & Ahmed, 2003). Overall, major ion concentrations were greater in the northeastern region than in the south (Fig. 2), suggesting the occurrence of intense water–rock interactions in the northeast.

Figure 3 shows a direct correlation between distance of mine and sampling sites, and quality parameters (positive groundwater flow). There was an overall

m-shaped tendency, with a rising trend upstream of the mine site and a decreasing trend downstream of the mine site, especially sodium, sulfate, and potassium quality parameters, indicating that it is possible the deterioration of the groundwater quality mainly on account of coal mining pollution significantly raised dissolution and mineralization of aquifer matrix (Zhang et al., 2022a, 2022b). Overall, these observations are in accordance with findings obtained by Yaqiang Li and Zhang (2022) from the Selian coal mining area of Inner Mongolia. The concentration of the quality parameters in the interval of 501–700m has increased, which may be related to the agricultural irrigation activities around the mine area. The combination of mine drainage into ditches, irrigation by farmers using water from the ditches, and

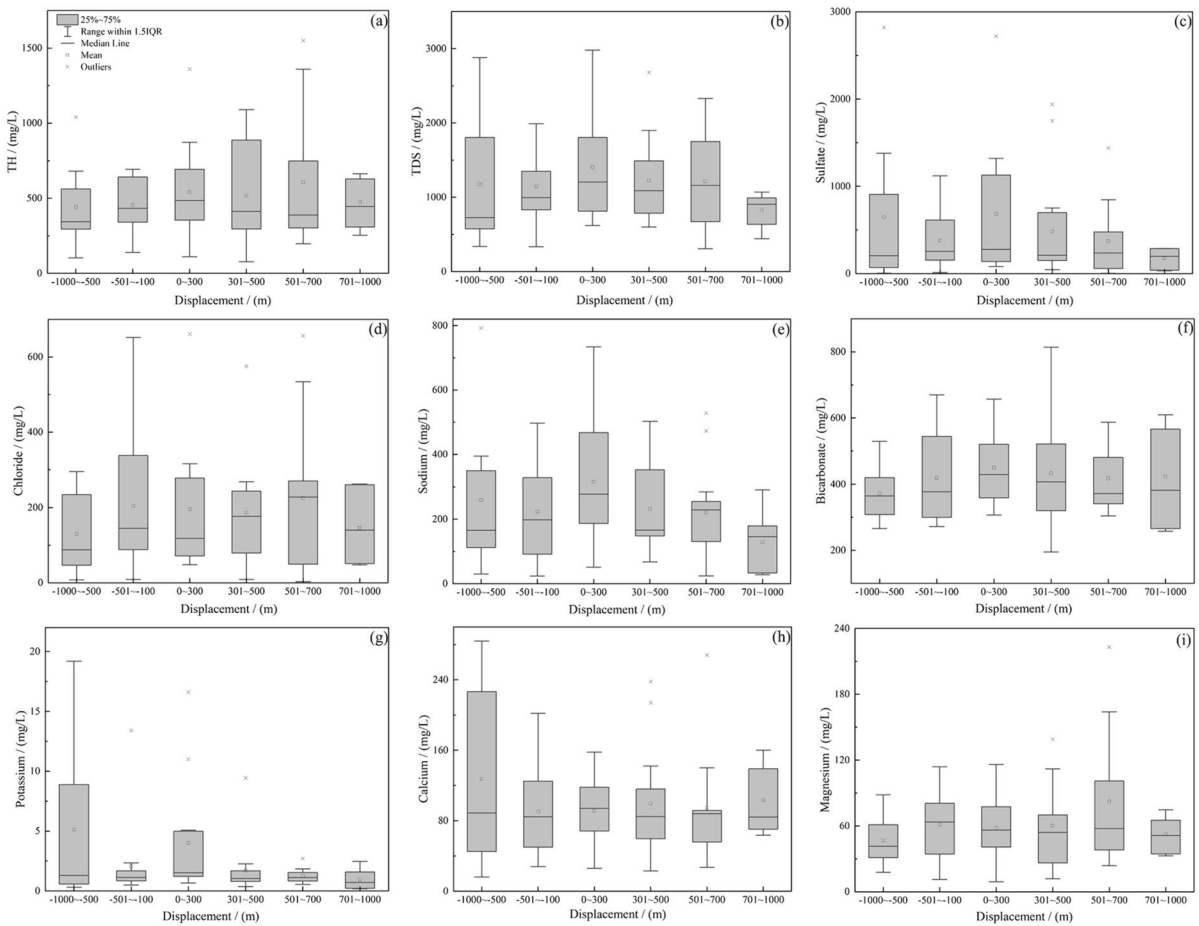


Fig. 3 Direct correlation between distance of mine and sampling sites, and quality parameters: **a** total hardness (TH), **b** total dissolved solids (TDS), **c** sulfate (SO_4^{2-}), **d** chloride

(Cl^-), **e** sodium (Na^+), **f** bicarbonate (HCO_3^-), **g** potassium (K^+), **h** calcium (Ca^{2+}), **i** magnesium (Mg^{2+})

accelerated groundwater flow from the mines may be the main reasons for the increase in pollution concentrations at this distance interval.

Ion correlation analysis

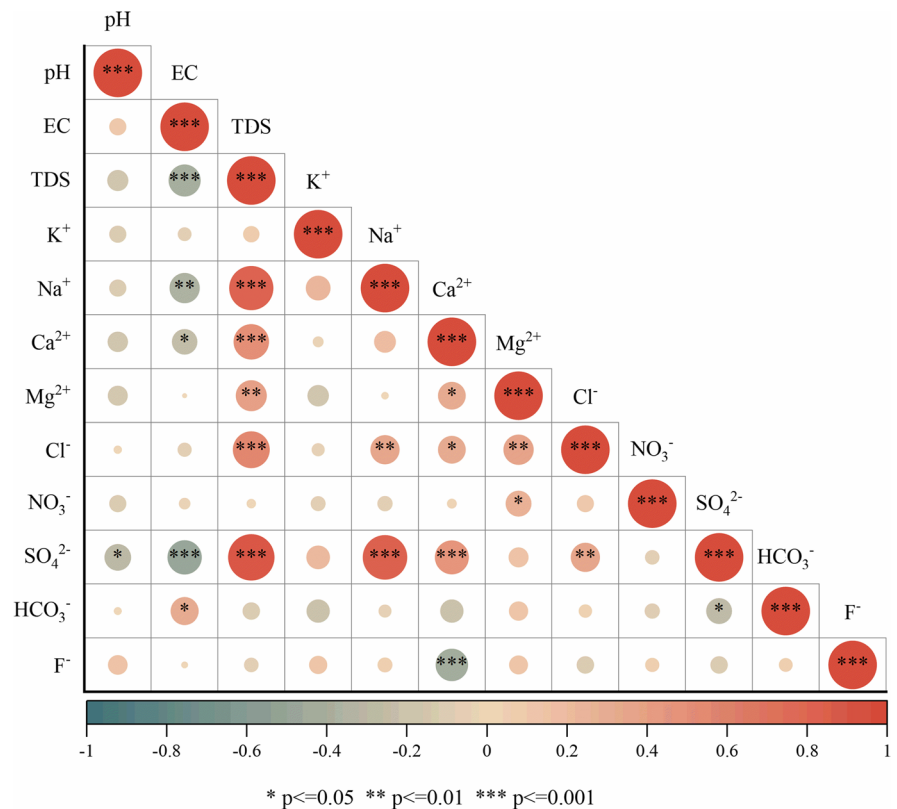
Figure 4 demonstrates the relationship of different groundwater ions, with different correlations between indicators. The correlation coefficient is simply a frequently utilized measure indicate how well one variable anticipates the other (Kumari & Rai, 2020). TH, TDS, SO_4^{2-} , Cl^- , Ca^{2+} , and Mg^{2+} , mutually showed a significant positive correlation ($p \leq 0.001$), demonstrating that they may have the same source or geochemical behavior (A. K. Tiwari et al., 2017). Carbonate dissolution, as well as halite and silicates weathering are important processes in the formation of hydrochemistry. The main composition of TDS is sodium, calcium and magnesium. The great correlation between Ca^{2+} and SO_4^{2-} suggests that primary source may be gypsum dissolution. (Tiwari et al., 2016). EC and TH, SO_4^{2-} , Na^+ , Ca^{2+} , and F^- had a

significant negative correlation ($p \leq 0.001$) (Subramani et al., 2005).

Principal component analysis

The principal component analysis method is predicated integration and simplification by retaining the maximum information of the original data, with reducing the calculation of unnecessary indicators and alleviating the workload. The SPSS principal component analysis function was adopted for principal factor extraction. After standardizing the original data, the correlation coefficients of each index were derived. Three principal component elements with eigenvalues of > 1 were extracted whose cumulative variance contribution reached 78.354% (Table S3). PC1 explained 46.977% of the total variance, and TDS, TH, SO_4^{2-} contributed to strong high positive loadings. This indicated the dissolution/precipitation of sulfate minerals. There were mid-high positive loadings for Cl^- , Na^+ , Ca^{2+} , indicating the dissolution of carbonate minerals (e.g., calcite, dolomite) and gypsum (Qian et al., 2016). PC1 generally indicated

Fig. 4 Correlation matrix of analyzed groundwater quality parameters



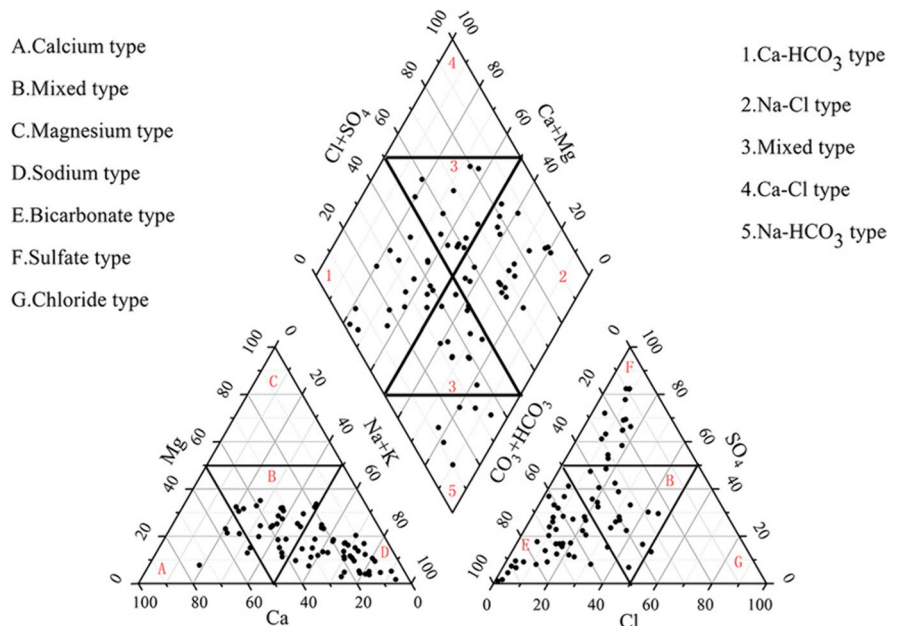
that water–rock interaction may be the main source of ions. PC2 explained 18.398% of the total variance. For F^- , it is possibly are result of the dissolution of fluorinated minerals. PC3 explained 12.980% of the variance, involving magnesium ions. Overall, the results of the PCA exhibited that dissolution/precipitation of minerals influenced the fairly complex hydrogeochemical characteristics of groundwater (Yuan et al., 2017).

Hydrochemical facies

Hydrochemical facies are defined as “denote the diagnostic chemical aspects of water solutions occurring in hydrologic systems,” indicating “the response of interrelated effects of the lithology and the pattern of ground-water flow” (Back, 1960). The Piper trilinear chart is a diagrammatic manifestation of water chemical data which is useful for identifying the types of groundwater hydrochemical based on chemical characteristics (Piper, 1944). One rhomb comprises the top of this diagram, with two triangles at the base. The major ions analyzed were unevenly distributed in the Piper diagram and further projected into the rhomb field to characterize the overall groundwater chemistry (Fig. 5). In the cation section, 35.21% of the groundwater points were in the center (zone B), reflecting insignificant governance of any particular

cation in the groundwater. 56.34% of the groundwater samples located in the bottom right margin (zone D), demonstrating the supremacy of sodium and potassium. The anion section showed that 53.52% of the groundwater points appeared in the bottom left margin (zone E), reflecting the dominance of bicarbonate which also shows that the carbonate and silicate weathering dominated lithology and had a large influence on the groundwater hydrochemistry. Meanwhile, a critical evaluation of the rhomb field showed that the water types were mainly into mixed type, calcium-bicarbonate type, sodium-chloride type, and sodium-bicarbonate type. Moreover, 18.31%+18.31% of the groundwater samples plunged in the center of the rhomb (zone 3) showing the mixed water types (calcium-magnesium-chloride-sulfate and calcium-sodium-bicarbonate) of the hydrochemistry, representing the sophisticated impact of anthropogenic activities, reverse ion exchange, as well as weathering. Of the groundwater samples, 25.35% were classified as a calcium-bicarbonate water type (zone 1). Infiltrated meteoric groundwater is frequently abundant in calcium and bicarbonate (Mukherjee & Singh, 2020; Sridharan & Nathan, 2018). Therefore, the existence of calcium-bicarbonate hydrochemistry facies indicated that the shallow groundwater aquifers are supplied with precipitation and integration of unfiltered meteoric water. About 29.58% of the

Fig. 5 Piper diagram for groundwater



samples appeared in the zone of the Na-Cl water type (zone 2), suggesting higher concentrations of sodium and chloride bearing salt. Few samples fell in the bottom of the rhomb (zone 5) and were categorized as the sodium-bicarbonate water type revealing the base ion exchange phenomena.

Sources of major ions and control mechanisms of hydrogeochemistry

The hydrogeochemical characteristics of groundwater may be controlled by diverse sources and processes in the aquifer, which can be analyzed by mathematical and graphical techniques (N. Rajmohan & Elango, 2004). In this study, the activity ratios of ions and the mineral phases saturation indices can be classified as a mathematical approach and Gibbs plots, respectively.

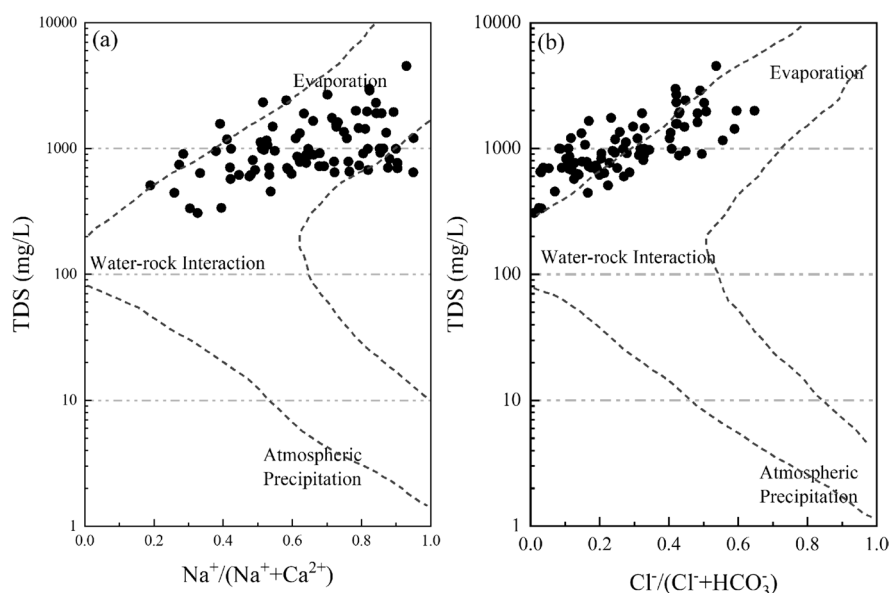
Hydrogeochemical processes and solute acquisition processes

Gibbs diagrams drafting major ion ratios (Na^+ / $(\text{Na}^+ + \text{Ca}^{2+})$) and $\text{Cl}^-/(\text{Cl}^- + \text{HCO}_3^-)$) and TDS plot groundwater samples were used to recognize and distinguish the functional sources of precipitation, mineral weathering, and evaporation function on the hydrochemistry of the research region groundwater (Fig. 6) (Gibbs, 1970; Natarajan Rajmohan et al.,

2021). As illustrated in the Gibbs diagram (Fig. 6), the cation ratios are situated from 0.19 to 0.95, as well as the anion ratios are from 0.01 to 0.65. The TDS value was high and samples were majority concentrated in the zone of evaporation and water-rock interaction. The major hydrogeochemical processes are of an interaction between weathered rock and groundwater in the area, and evaporative crystallization, with a slight impact from atmospheric precipitation.

The ion ratio coefficient (Fig. 7) can qualitatively determine the influence of different rock weathering in the region and trace the ion sources (Jie Zhang et al., 2022a, 2022b). The origin of sodium and potassium ions can be determined using the relationship between the ratio of $(\text{Na}^+ + \text{K}^+)/(\text{Cl}^-)$ (Fig. 7a). The $(\text{Na}^+ + \text{K}^+)/(\text{Cl}^-)$ ratio was approximately equal to one, which represents equivalent content of Na^+ and K^+ has been released through the dissolution of halite. This indicates that Na^+ and K^+ might have been derived from the dissolution of evaporite minerals, whereas a molar ratio of >1 is frequently defined as Na^+ and K^+ from a silicate weathering reaction, whereas the lower $(\text{Na}^+ + \text{K}^+)/(\text{Cl}^-)$ ratio (<1.0) may be attributed to an exchange of Na^+ for Ca^{2+} and Mg^{2+} in clays (Meybeck, 1987). Figure 7 a illustrates that the majority of the sample is located over the 1:1 line, with the ratio of $(\text{Na}^+ + \text{K}^+)/(\text{Cl}^-)$ generally ranging from 0.2 to 30.8. In a majority of samples,

Fig. 6 Gibbs diagram for groundwater



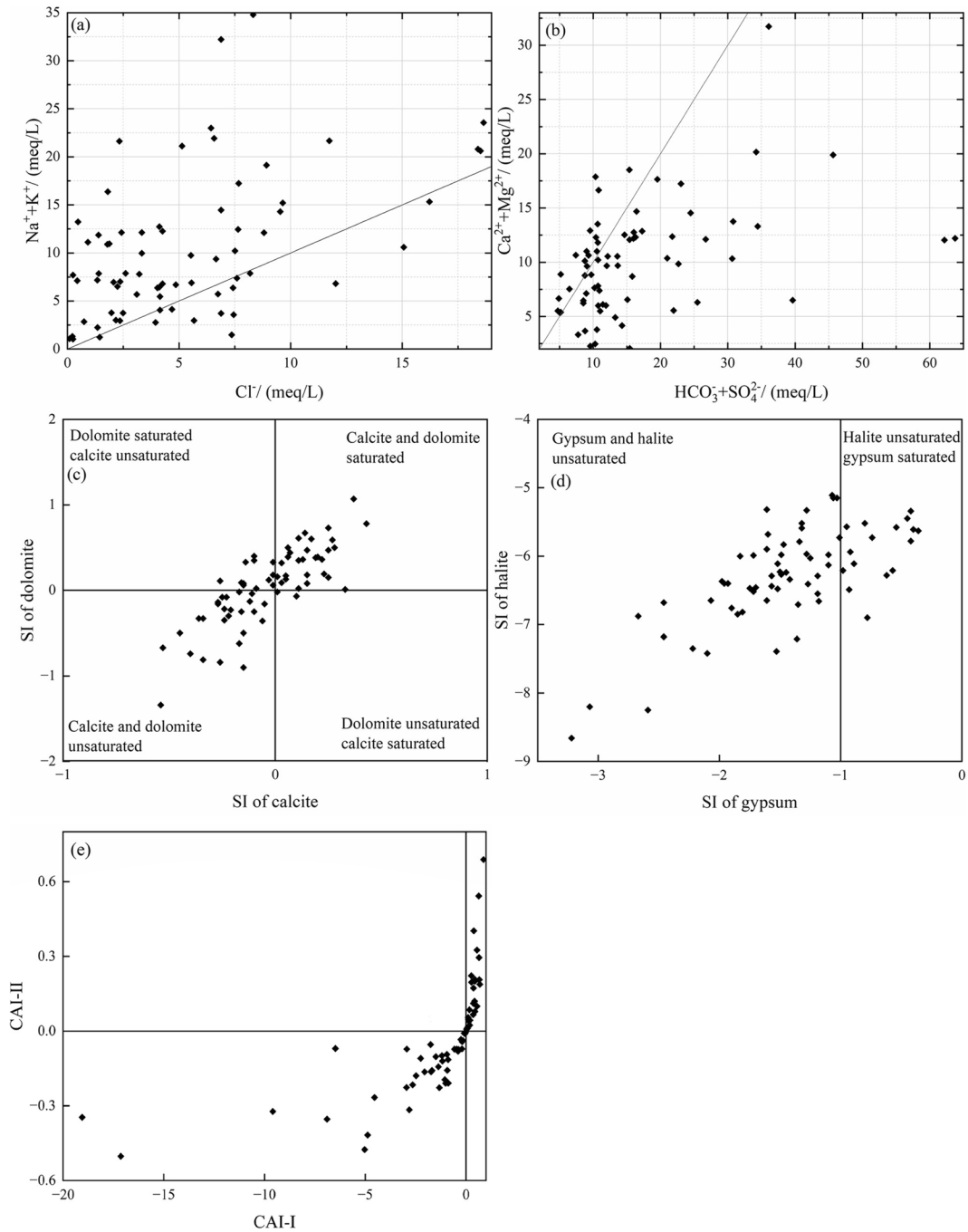


Fig. 7 Role of mineral weathering, evaporation processes, ion exchange reactions on water chemistry in this basin: **a** ($\text{Na}^+ + \text{K}^+$) versus (Cl^-), **b** ($\text{Ca}^{2+} + \text{Mg}^{2+}$) versus

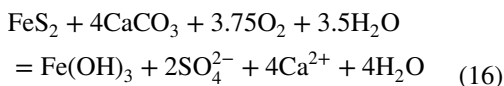
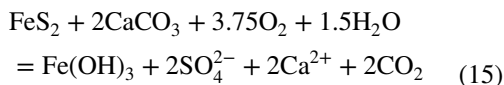
($\text{HCO}_3^- + \text{SO}_4^{2-}$), **c** saturation indices (SI) of calcite versus SI of dolomite, **d** SI of gypsum versus SI of halite, **e** CAI-I versus CAI-2

the Na^+ and K^+ concentration exceeded the chloride content, indicating a non-halite source and demonstrates the Na^+ and K^+ might have been originated

from silicate weathering, with only a finite contribution from atmospheric precipitation. The low content of K^+ in the area is attributed to its propensity to be

immobilized by clay minerals and to its engagement in the composition of secondary minerals (A. K. Tiwari et al., 2016).

If the main dominating processes in a system are the dissolution of gypsum and carbonate minerals, the plot of $(Ca^{2+} + Mg^{2+})$ versus $(HCO_3^- + SO_4^{2-})$ (Fig. 7b) will generate the perceived 1:1 ratio (N. Rajmohan & Elango, 2004). Furthermore, it is possible to explain a 1:1 link by the combination of pyrite oxidation and carbonate neutralization as a result of mining (Han et al., 2013).



As depicted in Fig. 7b, the ratio of $(Ca^{2+} + Mg^{2+}) / (HCO_3^- + SO_4^{2-})$ for the research area ranges from 0.1 to 1.7, numerous points stray from the 1:1 ratio and are clustered around and right of this line, which signifies a lack of Ca^{2+} and Mg^{2+} in this region, and excess HCO_3^- , SO_4^{2-} reflecting the control of ion exchange processes and rock weathering. A small number of samples fell under the equal line suggesting that reverse ion exchange or the dissolution of $CaCl_2$ and $MgCl_2$ minerals were the contributors of excess Ca^{2+} and Mg^{2+} .

The PHREEQC procedure is utilized to compute saturation indices (SI) of mineral phases which can identify the equilibrium condition of the water concerning a mineral phase (Garrels & Mackenzie, 1971). By utilizing SI from groundwater data without gathering solid phase specimens and interpreting the mineralogy, it is feasible to predict the reactive mineralogy of the subsurface (Deutsch, 1997). Saturation indices (SI) of calcite, dolomite, gypsum, and halite were calculated and graphed in Fig. 7c, d. If SI is positive, the groundwater is supersaturated involving a mineral, and it is subject to precipitate to the mineral phase of the solute load. Conversely, a negative SI specifies that there will be more mineral dissolution.

In the present study, the SI of calcite, dolomite, gypsum and rock salt are -0.54 to 0.43 , -1.34 to 1.07 , -3.22 to -0.36 , and -8.66 to -5.11 ,

respectively. Figure 7 c illustrates that regarding calcite and dolomite 46.5% and 60.6% of the points are oversaturated, while the remaining samples are unsaturated. Meanwhile, calcite and dolomite in these locations may continue to dissolve to increase the content of Ca^{2+} , Mg^{2+} , and HCO_3^- . As shown in Fig. 7d, in terms of groundwater, both gypsum and halite are unsaturated, which is a critical process in groundwater enhancing the content of SO_4^{2-} and Cl^- .

Cation exchange adsorption

The ion exchange process is also an essential controlling factor for groundwater chemistry in this region. Ion exchange and reverse ion exchange can be confirmed by chloro-alkaline indices (CAI) presented by Schoeller (1965), and expressed as (P. Li et al., 2014).

$$CAI - I = \frac{Cl^- - (Na^+ + K^+)}{Cl^-} \quad (17)$$

$$CAI - II = \frac{Cl^- - (Na^+ + K^+)}{SO_4^{2-} + HCO_3^- + CO_3^{2-} + NO_3^-} \quad (18)$$

A positive CAI expresses the presence of reverse ion exchange, in which magnesium and calcium in the aquifer material are exchanged for sodium and potassium from groundwater. The reaction is recognized as a cation–anion exchange reaction by negative CAI. The degree of exchange can be judged from the absolute value of the CAI, and the larger value in terms of its absolute value, the more likely the reaction will occur. Figure 7 e illustrates that the CAI-1 and CAI-2 vary from -19.05 to 0.86 and -0.50 to 0.69 , respectively. About 62.0% of points had positive values demonstrating a chloro-alkaline disequilibrium whilst the interaction qua a base–exchange reaction. In 38.0% of the groundwater, the results showed negative values, revealing that ion exchange is predominant; videlicet, a swap of Ca^{2+} and Mg^{2+} in groundwater with the Na^+ in aquifer material (N. Rajmohan & Elango, 2004).

Assessment of groundwater quality for agricultural suitability

Irrigation water quality affects crop growth. Thus, it is critical to study irrigation water quality, as excessive salinity and alkalinity can lead to salinization of the land, and affect crop yield and quality. Irrigation water quality is evaluated using various single indicators (Ayers & Westcot, 1985; Yu et al., 2020). Table 1 shows the irrigation quality indicators.

Na% and SAR are essential indicators for assessing the applicability of groundwater for irrigation (Wilcox, 1955), which expresses a sodium or alkali hazard. A high Na⁺ content result in formation of an alkaline soil, and cation exchange adsorption. Sodium ions displacing Mg²⁺ and Ca²⁺ ions are absorbed by clay particles, reducing infiltration, consequently resulting in hard soil with inefficient inside drainage (Saleh et al., 1999; A. Tiwari et al., 2013). Na% ranged between 18.43 and 93.40%, with an average of 54.59%. Thirty sampling points exceeded the standard limits, accounting for 42.25%. The SAR values ranged from 3.55 to 118.25, with 59.15% of the sampling points unsuitable for irrigation and 42.25% of the groundwater had extremely sodium hazard.

Residual sodium carbonate (RSC) values are also used to characterize the degree of alkali damage (Laboratory, 1954). Positive values represent the presence of carbonate and bicarbonate in water reacting with sodium ions, causing alkali damage, while negative values reflect the opposite. The higher the value indicates that it is more likely to cause alkali damage. Table 1 shows values ranging from -119 to 608.5, with a mean value of 262.33 and a large exceedance of 92.96%, indicating that the sampling area is unsuitable for irrigation and alkaline soil exists.

MH is defined as the inordinate amount of magnesium above Ca and Mg. Excess Mg influences soil quality, bringing about unfavorable agricultural rewards (Szabolcs, 1964). A MH ratio > 50% is

recognized as detrimental and inappropriate for irrigation. Of the sampling points in the region, 28.9% had a MH value over 50% and were undesirable for irrigation.

The values of KR are critical factors for evaluating the quality of agricultural water. The values varied from 0.21 to 14.09, and 60.61% of the KR is unsuitable for irrigation.

Spatial distribution map of the irrigation water quality (Fig. 8) was generated by carrying out water quality index (WQI) via a comprehensive weighting model based on AHP-CRITIC integrating various single indicators and combining IDW technology in GIS. Based on this, the study area was broadly classified into three categories: appropriate zone (less constraint), moderately appropriate zone (moderate constraint), and inappropriate zone (severe constraint). The results have demonstrated that the central part and southeastern of the study area showed high suitability zone accounting for nearly 43.17%, in the western portion of the study area showed moderate suitability zone accounting for nearly 18.85% which need careful irrigation. In contrast, the upper part of the study area occupying 37.98% had very unsuitable water for irrigation and extremely poor water quality, which was caused by various sources, including intensive agricultural activities, densely populated living areas, especially richly historied industrial activities such as mining. Overall, the study area was dominated by high suitability areas for irrigation, and water quality safety in some areas requires careful consideration.

Discussion

The degradation of the groundwater quality mainly on account of coal mining pollution significantly raised dissolution and mineralization of aquifer matrix. The research area is located in an area with

Table 1 Irrigation quality indices

Index	Minimum	Maximum	Mean	Standard deviation	Permissible limit	Exceeding rate
Na%	18.43	93.40	54.59	19.75	≤ 60	42.25%
SAR	3.55	118.25	28.33	21.67	≤ 18	59.15%
RSC	-119.00	608.50	262.33	152.78	≤ 2.5	92.96%
MH	9.58	66.67	38.92	13.39	≤ 50	28.79%
KR	0.21	14.09	1.90	2.13	≤ 1.0	60.61%

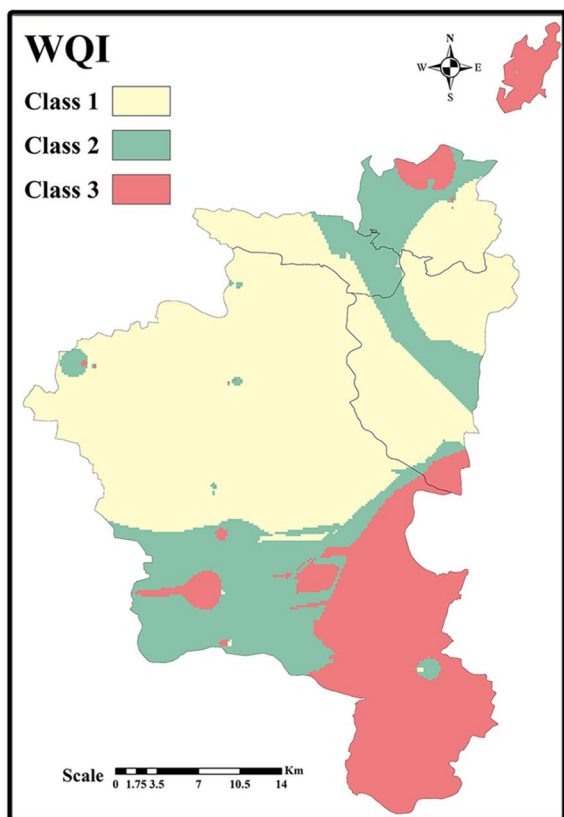


Fig. 8 Spatial distribution of the Water Quality Index (WQI) for the groundwater in the region (Class 1: good irrigation water quality; Class 2: permissible irrigation water quality; Class 3: useless for use as irrigation water)

a concentration of coal mining, and which in totality reflects a high concentration in the north of China. The groundwater exhibits high salinity, high alkalinity, and almost neutral pH, which is a distinctive feature of the mining area (Mansilha et al., 2021). During coal mining, the original strata and water flow channel are affected and destroyed in the aquifer surrounding the deposit, leading to a weakening of the aquifer. A roadway forms centered on the pressure drop funnel, exacerbating water–rock action during mine water migration, resulting in the generation and release of pollutants. Moreover, the mining changes the original reduction environment and replaces a closed system with an open or semi-open system in groundwater of the coal mining region. Under the combined action of air, water and bacteria, nodular siderite and pyrite (primarily pyrite) in the coal form acid mine wastewater (Burri et al., 2019), which

penetrates into the groundwater system through irrigation flow back and channel cracks and pores, leading to contamination of the ambient groundwater. In addition, the long exposure of unwanted and uneconomic materials dumped near mines are exposed to rain or other surficial water, which also leads to the leaching of pollution, which in turn causes a potential threat to groundwater safety.

The pH of groundwater affected by acid mine wastewater is generally weakly acidic. As an example, the pH range of spring water samples around the Onzawa mine in Akita Prefecture, Japan was 6.3–6.7 (Nishimoto et al., 2021). The acid groundwater in Figueira city, Paraná State, Brazil (Galhardi & Bonotto, 2016), was probably attributed to acid mine drainage generation and infiltration, resulting in pH values in the range of 2.94–6.63. Variance to the observations of previous studies about the low pH in groundwater, it is notable that our findings reflected an almost neutral pH. A popular explanation is the insufficiency of pyrites in particular layers and the preponderance of carbonate minerals (Singh, 1988). The share of carbonate minerals in the main mining horizon of the region comprised 40–90%, and thus, may constitute a reasonable justification.

The research area is positioned in the regional watershed, surface water systems are scarce, so the principal source of provision is groundwater. However, the drastic increase in water costs is around 61% of the entire region's agricultural irrigation areas and underdevelopment of regional surface water results in the use of unconventional free water sources. Unfortunately, water of marginal value, such as groundwater influenced by coal mining, is often considered a possible choice in agriculture. The consequences of impacted adjacent water bodies and farmland over 10 km from its origins are brought by permanent and unregulated use of contaminated water, apparently lead to decreasing crop yields, degradation of soil characteristics, and serious environmental and health damage. In Highveld coal fields that introduced acidic water into the groundwater system, rivers and marshes for decades have recorded SO_4^{2-} values over 7000 mg/L and $\text{pH} < 2$ (Burri et al., 2019).

The results in this research demonstrated that irrigation indicators data for this coal gathering area have unacceptable index values, and the quality is affected by high salinity and alkalinity, requiring careful consideration of irrigation activities. If the soil is

satisfactory in terms of leaching and drainage, irrigation is feasible. Alternatively, the impact can be prevented by designing effective pre-treatment methods to reduce groundwater salinity and alkalinity, such as ion exchange, membrane separation, electro dialysis, precipitation, reverse osmosis and adsorption, or the selection of plants with good salt tolerance to reduce the risk of salinity damage.

Conclusions

This study provided a deep analysis of 71 shallow groundwater samples near 12 coal mines in the Huai-bei Plain. Conventional hydrochemistry methods and principal component analysis were utilized to investigate the hydrogeochemical characteristics and controlling factors of these groundwater samples. Additionally, an evaluation of irrigation suitability was also conducted through the implementation of the AHP-CRITIC integrated weighting method.

- The concentrations of TH, TDS, SO_4^{2-} , Na^+ , F^- were higher than the allowable limit (groundwater class III water standard) and the over-standard rates were 40.85%, 43.66%, 40.85%, 46.48%, and 64.79%, respectively. Major ion concentrations were greater in the northeastern region than in the southern region. Meanwhile, the groundwater quality was more deteriorated as the sampling point was closer to the field of coal mine. Majority of groundwater samples are dominated by Ca-HCO_3 , Na-Cl , and the mixed type. The ion ratio coefficient and PCA revealed that water-rock interaction was the main process controlling groundwater chemistry. Mining activities can accelerate water-rock interactions and affect water quality.
- According to groundwater irrigation suitability zonation map, the study area was dominated by high suitability irrigation zones occupying 43.17% of the area, while moderate and medium suitability zones occupy 18.85% and 37.98%, respectively. The high-salinity and alkalinity of groundwater in this study area may originate from the enhanced dissolution and mineralization of water-rock interactions and leakage of acid mine wastewater, due to mining and the sampling time located in the winter season when freshwater is scarce. Hence, proper treatment of groundwater,

adequate drainage installation and salt-tolerance cropping patterns are needed to mitigate suitability limitation for irrigation purpose.

Author contribution All authors contributed to the study conception and design and all authors commented on previous versions of the manuscript. All authors read and approved the final manuscript. Y.T. designed the study, collected, processed, and prepared samples used in the experiments, performed all statistical analyses, and drafted the manuscript. Q.L. helped design the study, provided scientific input and guidance, assisted in sample collection, revised the manuscript, and provided comments and corrections. Y.J. assisted in sample collection, reviewed, and revised the manuscript, and provided comments and corrections. Q.D. reviewed, revised the manuscript, and provided comments and corrections. Y.L. developed the project, assisted with study design, secured and oversaw funding, provided scientific input and guidance, revised the manuscript, and provided comments and corrections. J.S. developed the project, assisted with study design, secured and oversaw funding, provided scientific input and guidance, revised the manuscript, and provided comments and corrections.

Funding This research was supported by National R&D Program of China (2023YFC3708700).

Data availability Raw data that support the findings of this study are available from the corresponding author, upon reasonable request.

Declarations

Ethics approval Not applicable.

Competing interests The authors declare no competing interests.

References

- Abdelkarim, B., Telahigue, F., Abaab, N., Boudabra, B., & Agoubi, B. (2023). AHP and GIS for assessment of groundwater suitability for irrigation purpose in coastal-arid zone: Gabes region, southeastern Tunisia. *Environmental Science and Pollution Research*, 30(6), 15422–15437.
- Adimalla, N., & Qian, H. (2019). Groundwater quality evaluation using water quality index (WQI) for drinking purposes and human health risk (HHR) assessment in an agricultural region of Nanganur, south India. *Ecotoxicology and Environmental Safety*, 176, 153–161.
- Adimalla, N., & Qian, H. (2021). Groundwater chemistry, distribution and potential health risk appraisal of nitrate enriched groundwater: A case study from the semi-urban region of South India. *Ecotoxicology and Environmental Safety*, 207, 111277.

- Ayers, R. S., & Westcott, D. W. (1985). *Water quality for agriculture* (Vol. 29): Food and Agriculture Organization of the United Nations Rome.
- Back, W. (1960). Hydrochemical facies and ground-water flow patterns in Northern Atlantic Coastal Plain. *AAPG Bulletin*, 44(7), 1244–1245.
- Bauder, T. A., Waskom, R., Sutherland, P., Davis, J., Follett, R., & Soltanpour, P. (2011). Irrigation water quality criteria. *Service in action*; no. 0.506.
- Bortolini, L., Maucieri, C., & Borin, M. (2018). A tool for the evaluation of irrigation water quality in the arid and semi-arid regions. *Agronomy*, 8(2), 23.
- Burri, N. M., Weatherl, R., Moeck, C., & Schirmer, M. (2019). A review of threats to groundwater quality in the anthropocene. *Science of the Total Environment*, 684, 136–154.
- Chemura, A., Kutwayo, D., Chagwasha, T. M., & Chidoko, P. (2014). An assessment of irrigation water quality and selected soil parameters at mutema irrigation scheme, Zimbabwe. *Journal of Water Resource and Protection*, 2014.
- Chowdhury, P., Mukhopadhyay, B. P., & Bera, A. (2022). Hydrochemical assessment of groundwater suitability for irrigation in the north-eastern blocks of Purulia district, India using GIS and AHP techniques. *Physics and Chemistry of the Earth*, 126, 17. <https://doi.org/10.1016/j.pce.2022.103108>
- Dalin, Carole, Kastner, Thomas, Wada, Yoshihide, . . . J. (2017). Groundwater depletion embedded in international food trade. *Nature*, 543(Mar.30 TN.7647), 700–704.
- de Graaf, I. E., Gleeson, T., Sutanudjaja, E. H., & Bierkens, M. F. (2019). Environmental flow limits to global groundwater pumping. *Nature*, 574(7776), 90–94.
- Deutsch, W. (1997). *Groundwater geochemistry: Fundamentals and application to contamination*. CRC.
- Dhaouadi, L., Besser, H., Karbout, N., Khaldi, R., Haj-Amor, Z., Maachia, S., & Ouassar, F. (2022). Environmental sensitivity and risk assessment in the Saharan Tunisian oasis agro-systems using the deepest water table source for irrigation: Water quality and land management impacts. *Environment, Development and Sustainability*, 24(9), 10695–10727.
- Elvis, B. W. W., Arsene, M., Theophile, N. M., Bruno, K. M. E., & Olivier, O. A. (2022). Integration of Shannon entropy (SE), frequency ratio (FR) and analytical hierarchy process (AHP) in GIS for suitable groundwater potential zones targeting in the Yoyo river basin, Meiganga area Adamawa Cameroon. *Journal of Hydrology-Regional Studies*, 39, 24. <https://doi.org/10.1016/j.ejrh.2022.100997>
- Fetter, C. (1990). *Applied hydrogeology* (2nd Edn., 592 p.). New Delhi: CBS Publishers and Distributors. Gibbs, R.J. (1970). Mechanisms controlling world water chemistry. *Science*, 170(3962), 1088–1090.
- Freeze, R., & Cherry, J. (1979). Ground water contamination. *Groundwater. Ontario. Canada*, 383–456.
- Galhardi, J. A., & Bonotto, D. M. (2016). Hydrogeochemical features of surface water and groundwater contaminated with acid mine drainage (AMD) in coal mining areas: A case study in southern Brazil. *Environmental Science and Pollution Research*, 23(18), 18911–18927.
- Garrels, R. M., & Mackenzie, F. T. (1971). Gregor's denudation of the continents. *Nature*, 231(5302), 382–383
- Gibbs, R. J. (1970). Mechanisms controlling world water chemistry. *Science*, 170(3962), 1088–1090.
- Gidey, A. (2018). Geospatial distribution modeling and determining suitability of groundwater quality for irrigation purpose using geospatial methods and water quality index (WQI) in Northern Ethiopia. *Applied Water Science*, 8(3). <https://doi.org/10.1007/s13201-018-0722-x>
- Haldar, K., Kujawa-Roeleveld, K., Dey, P., Bosu, S., Datta, D. K., & Rijnaarts, H. H. M. (2020). Spatio-temporal variations in chemical-physical water quality parameters influencing water reuse for irrigated agriculture in tropical urbanized deltas. *Science of the total environment*, 708. <https://doi.org/10.1016/j.scitotenv.2019.134559>
- Han, Y., Wang, G., Cravotta, C. A., III., Hu, W., Bian, Y., Zhang, Z., & Liu, Y. (2013). Hydrogeochemical evolution of Ordovician limestone groundwater in Yanzhou North China. *Hydrological Processes*, 27(16), 2247–2257.
- He, X., Li, P., Wu, J., Wei, M., Ren, X., & Wang, D. (2021). Poor groundwater quality and high potential health risks in the Datong Basin, northern China: Research from published data. *Environmental Geochemistry and Health*, 43(2), 791–812.
- Hubert, E., & Wolkersdorfer, C. (2015). Establishing a conversion factor between electrical conductivity and total dissolved solids in South African mine waters. *Water Sa*, 41(4), 490–500.
- Keqiang, H., Lu, G., Yuanyuan, G., Huilai, L., & Yongping, L. (2019). Research on the effects of coal mining on the karst hydrogeological environment in Jiaozuo mining area China. *Environmental Earth Sciences*, 78(15), 1–13.
- Khalid, S. (2019). An assessment of groundwater quality for irrigation and drinking purposes around brick kilns in three districts of Balochistan province, Pakistan, through water quality index and multivariate statistical approaches. *Journal of Geochemical Exploration*, 197, 14–26.
- Kumari, M., & Rai, S. (2020). Hydrogeochemical evaluation of groundwater quality for drinking and irrigation purposes using water quality index in semi arid region of India. *Journal of the Geological Society of India*, 95(2), 159–168.
- Laboratory, R. S. (1954). *Diagnosis and improvement of saline and alkali soils*: US Department of Agriculture.
- Li, P., Wu, J., Qian, H., Lyu, X., & Liu, H. (2014). Origin and assessment of groundwater pollution and associated health risk: A case study in an industrial park, northwest China. *Environmental Geochemistry and Health*, 36(4), 693–712.
- Li, P., Wu, J., Qian, H., Zhang, Y., Yang, N., Jing, L., & Yu, P. (2016). Hydrogeochemical characterization of groundwater in and around a wastewater irrigated forest in the southeastern edge of the Tengger Desert Northwest China. *Exposure and Health*, 8(3), 331–348.
- Li, P., Wu, J., Tian, R., He, S., He, X., Xue, C., & Zhang, K. (2018). Geochemistry, hydraulic connectivity and quality appraisal of multilayered groundwater in the Hongdunzi Coal Mine, Northwest China. *Mine Water and the Environment*, 37(2), 222–237.
- Li, Y., Wei, M. L., Liu, L., Yu, B. W., Dong, Z. W., & Xue, Q. (2021). Evaluation of the effectiveness of VOC-contaminated soil preparation based on AHP-CRITIC-TOPSIS model. *Chemosphere*, 271, 11. <https://doi.org/10.1016/j.chemosphere.2021.129571>

- Li, Y., & Zhang, X. (2022). Characterization of the health and irrigation risks and hydrochemical properties of groundwater: a case study of the Selian coal mine area, Ordos, Inner Mongolia. *Applied Water Science*, 12(10). <https://doi.org/10.1007/s13201-022-01762-9>
- Liu, J., Peng, Y., Li, C., Gao, Z., & Chen, S. (2021). Characterization of the hydrochemistry of water resources of the Weibei Plain, Northern China, as well as an assessment of the risk of high groundwater nitrate levels to human health. *Environmental Pollution*, 268, 115947.
- Mansilha, C., Melo, A., Flores, D., Ribeiro, J., Rocha, J. R., Martins, V., . . . Espinha Marques, J. (2021). Irrigation with Coal Mining Effluents: Sustainability and Water Quality Considerations (São Pedro da Cova, North Portugal). *Water*, 13(16), 2157.
- Menció, A., Folch, A., & Mas-Pla, J. (2012). Identifying key parameters to differentiate groundwater flow systems using multifactorial analysis. *Journal of Hydrology*, 472, 301–313.
- Meybeck, M. (1987). Global chemical weathering of surficial rocks estimated from river dissolved loads. *American Journal of Science*, 287(5), 401–428.
- Moore, P. J., Martin, J. B., & Sreaton, E. J. (2009). Geochemical and statistical evidence of recharge, mixing, and controls on spring discharge in an eogenetic karst aquifer. *Journal of Hydrology*, 376(3–4), 443–455.
- Moya, C. E., Raiber, M., Taulis, M., & Cox, M. E. (2015). Hydrochemical evolution and groundwater flow processes in the Galilee and Eromanga basins, Great Artesian Basin, Australia: A multivariate statistical approach. *Science of the Total Environment*, 508, 411–426.
- Mukherjee, I., & Singh, U. K. (2020). Fluoride abundance and their release mechanisms in groundwater along with associated human health risks in a geologically heterogeneous semi-arid region of east India. *Microchemical Journal*, 152, 104304.
- Nishimoto, N., Yamamoto, Y., Yamagata, S., Igarashi, T., & Tomiyama, S. (2021). Acid Mine Drainage Sources and Impact on Groundwater at the Osarizawa Mine Japan. *Minerals*, 11(9), 998.
- Nordstrom, D. K., Blowes, D. W., & Ptacek, C. J. (2015). Hydrogeochemistry and microbiology of mine drainage: An update. *Applied Geochemistry*, 57, 3–16.
- Peterson, B. J., Wollheim, W. M., Mulholland, P. J., Webster, J. R., Meyer, J. L., Tank, J. L., . . . Hershey, A. E. (2001). Control of nitrogen export from watersheds by headwater streams. *Science*, 292(5514), 86–90.
- Piper, A. M. (1944). A graphic procedure in the geochemical interpretation of water-analyses. *Eos, Transactions American Geophysical Union*, 25(6), 914–928.
- Qian, J., Wang, L., Ma, L., Lu, Y., Zhao, W., & Zhang, Y. (2016). Multivariate statistical analysis of water chemistry in evaluating groundwater geochemical evolution and aquifer connectivity near a large coal mine, Anhui China. *Environmental Earth Sciences*, 75(9), 1–10.
- Qiu, H. L., Gui, H. R., Xu, H. F., Cui, L., & Yu, H. (2023). Occurrence, controlling factors and noncarcinogenic risk assessment based on Monte Carlo simulation of fluoride in mid-layer groundwater of Huaibei mining area, North China. *Science of the Total Environment*, 856, 10. <https://doi.org/10.1016/j.scitotenv.2022.159112>
- Rajkumar, H., Naik, P. K., & Rishi, M. S. (2022). A comprehensive water quality index based on analytical hierarchy process. *Ecological Indicators*, 145, 19. <https://doi.org/10.1016/j.ecolind.2022.109582>
- Rajmohan, N., & Elango, L. (2004). Identification and evolution of hydrogeochemical processes in the groundwater environment in an area of the Palar and Cheyyar River Basins Southern India. *Environmental Geology*, 46(1), 47–61. <https://doi.org/10.1007/s00254-004-1012-5>
- Rajmohan, N., Masoud, M. H. Z., & Niyazi, B. A. M. (2021). Impact of evaporation on groundwater salinity in the arid coastal aquifer, Western Saudi Arabia. *Catena*, 196. <https://doi.org/10.1016/j.catena.2020.104864>
- Redwan, M., Abdel Moneim, A. A., & Amra, M. A. (2016). Effect of water–rock interaction processes on the hydrogeochemistry of groundwater west of Sohag area Egypt. *Arabian Journal of Geosciences*, 9(2), 1–14.
- Rodríguez-Lado, L., Sun, G., Berg, M., Zhang, Q., Xue, H., Zheng, Q., & Johnson, C. A. (2013). Groundwater arsenic contamination throughout China. *Science*, 341(6148), 866–868.
- Rowell, D. L. (2014). *Soil science: Methods & applications*: Routledge.
- Saber, M., Mokhtar, M., Bakheit, A., Elfeky, A. M., Gameh, M., Mostafa, A., . . . Hamada, A. (2022). An integrated assessment approach for fossil groundwater quality and crop water requirements in the El-Kharga Oasis, Western Desert, Egypt. *Journal of Hydrology-Regional Studies*, 40, 21. <https://doi.org/10.1016/j.ejrh.2022.101016>
- Sajedi-Hosseini, F., Malekian, A., Choubin, B., Rahmati, O., Cipullo, S., Coulon, F., & Pradhan, B. (2018). A novel machine learning-based approach for the risk assessment of nitrate groundwater contamination. *Science of the Total Environment*, 644, 954–962.
- Saleh, A., Al-Ruwaih, F., & Shehata, M. (1999). Hydrogeochemical processes operating within the main aquifers of Kuwait. *Journal of Arid Environments*, 42(3), 195–209.
- Saxena, V. K., & Ahmed, S. (2003). Inferring the chemical parameters for the dissolution of fluoride in groundwater. *Environmental Geology*, 43(6), 731–736. <https://doi.org/10.1007/s00254-002-0672-2>
- Schoeller, H. (1965). *Qualitative evaluation of groundwater resources* (p. 5483). UNESCO.
- Schroeder, W., Holy, M., Pesch, R., Harmens, H., Fagerli, H., Alber, R., . . . Zechmeister, H. G. (2010). First Europe-wide correlation analysis identifying factors best explaining the total nitrogen concentration in mosses. *Atmospheric Environment*, 44(29), 3485–3491. <https://doi.org/10.1016/j.atmosenv.2010.06.024>
- Sengupta, P. (2013). Potential Health Impacts of Hard Water. *International Journal of Preventive Medicine*, 4(8), 866–875.
- Sheng, D., Meng, X., Wen, X., Wu, J., Yu, H., & Wu, M. (2022). Contamination characteristics, source identification, and source-specific health risks of heavy metal (loid)s in groundwater of an arid oasis region in Northwest China. *Science of the Total Environment*, 841, 156733.

- Siddique, J., Shahab, A., Azeem, T., Bangash, A. A., Naseem, A. A., Riaz, O., . . . Rehman, Q. U. (2022). Hydrochemical appraisal of fluoride contamination in groundwater and human health risk assessment at Isa Khel, Punjab, Pakistan. *Environmental Technology & Innovation*, 27, 13. <https://doi.org/10.1016/j.eti.2022.102445>
- Singh, G. (1988). Impact of coal mining on mine water quality. *International Journal of Mine Water*, 7(3), 49–59.
- Sridharan, M., & Nathan, D. S. (2018). Chemometric tool to study the mechanism of arsenic contamination in groundwater of Puducherry Region, South East Coast of India. *Chemosphere*, 208, 303–315.
- Srinivasamoorthy, K., Vasanthavigar, M., Chidambaram, S., Anandhan, P., Manivannan, R., & Rajivgandhi, R. (2012). Hydrochemistry of groundwater from Sarabanga minor basin, Tamilnadu, India. *Proceedings of the International Academy of Ecology and Environmental Sciences*, 2(3), 193.
- Subramani, T., Elango, L., & Damodarasamy, S. R. (2005). Groundwater quality and its suitability for drinking and agricultural use in Chithar River Basin, Tamil Nadu India. *Environmental Geology*, 47(8), 1099–1110. <https://doi.org/10.1007/s00254-005-1243-0>
- Sunkari, E. D., Seidu, J., & Ewusi, A. (2022). Hydrogeochemical evolution and assessment of groundwater quality in the Togo and Dahomeyan aquifers, Greater Accra Region Ghana. *Environmental Research*, 208, 112679.
- Szabolcs, I. (1964). The influence of irrigation water of high sodium carbonate content on soils. *Agrokémia és talajtan*, 13(sup), 237–246.
- Tessema, S., Mirgorodsky, D., Merten, D., Hildebrandt, A., Attinger, S., & Büchel, G. (2013). Hydrochemical characterization of groundwater system of biodiversity experimental field: Jena Germany. *Environmental Earth Sciences*, 70(2), 821–837.
- Tiwari, A., Mahato, M., & Singh, A. (2013). Quality assessment and suitability for irrigation uses of surface water of Pratapgarh district. *Indian Journal Environmental Protection*, 33(5), 370–378.
- Tiwari, A. K., De Maio, M., Singh, P. K., & Singh, A. K. (2016). Hydrogeochemical characterization and groundwater quality assessment in a coal mining area, India. *Arabian Journal of Geosciences*, 9(3). <https://doi.org/10.1007/s12517-015-2209-5>
- Tiwari, A. K., Singh, A. K., Singh, A. K., & Singh, M. P. (2017). Hydrogeochemical analysis and evaluation of surface water quality of Pratapgarh district, Uttar Pradesh India. *Applied Water Science*, 7(4), 1609–1623. <https://doi.org/10.1007/s13201-015-0313-z>
- Wang, J., Liu, G., Liu, H., & Lam, P. K. (2017). Multivariate statistical evaluation of dissolved trace elements and a water quality assessment in the middle reaches of Huaihe River, Anhui, China. *Science of the Total Environment*, 583, 421–431.
- Wilcox, L. (1955). *Classification and use of irrigation waters*: US Department of Agriculture.
- Wu, J., Li, P., & Qian, H. (2015). Hydrochemical characterization of drinking groundwater with special reference to fluoride in an arid area of China and the control of aquifer leakage on its concentrations. *Environmental Earth Sciences*, 73(12), 8575–8588.
- Wu, J., Zhou, H., He, S., & Zhang, Y. (2019). Comprehensive understanding of groundwater quality for domestic and agricultural purposes in terms of health risks in a coal mine area of the Ordos basin, north of the Chinese Loess Plateau. *Environmental Earth Sciences*, 78(15), 1–17.
- Wu, Z. S., Lai, X. J., & Li, K. Y. (2021). Water quality assessment of rivers in Lake Chaohu Basin (China) using water quality index. *Ecological Indicators*, 121, 8. <https://doi.org/10.1016/j.ecolind.2020.107021>
- Xiao, L. L., Li, F., Niu, C., Dai, G. L., Qiao, Q., & Lin, C. S. (2023). Evaluation of water inrush hazard in coal seam roof based on the AHP-CRITIC composite weighted method. *Energies*, 16(1), 20. <https://doi.org/10.3390/en16010114>
- Yadav, S., Irfan, M., Ahmad, A., & Hayat, S. (2011). Causes of salinity and plant manifestations to salt stress: A review. *Journal of Environmental Biology*, 32(5), 667.
- Yang, Q., Li, Z., Ma, H., Wang, L., & Martín, J. D. (2016). Identification of the hydrogeochemical processes and assessment of groundwater quality using classic integrated geochemical methods in the Southeastern part of Ordos basin, China. *Environmental Pollution*, 218, 879–888.
- Yu, H., Gui, H., Zhao, H., Wang, M., Li, J., Fang, H., . . . Zhang, Y. (2020). Hydrochemical characteristics and water quality evaluation of shallow groundwater in Suxian mining area, Huaibei coalfield, China. *International Journal of Coal Science & Technology*, 7(4), 825–835.
- Yuan, J., Xu, F., Deng, G., Tang, Y., & Li, P. (2017). Hydrogeochemistry of Shallow Groundwater in a Karst Aquifer System of Bijie City, Guizhou Province. *Water*, 9(8). <https://doi.org/10.3390/w9080625>
- Zaman, M., Shahid, S. A., & Heng, L. (2018). Irrigation water quality *Guideline for salinity assessment, mitigation and adaptation using nuclear and related techniques* (pp. 113–131): Springer.
- Zhai, Y., Han, Y., Lu, H., Du, Q., Xia, X., Teng, Y., . . . Wang, J. (2022). Interactions between anthropogenic pollutants (biodegradable organic nitrogen and ammonia) and the primary hydrogeochemical component Mn in groundwater: Evidence from three polluted sites. *Science of the total environment*, 808, 152162.
- Zhang, Y., Shi, P., Li, F., Wei, A., Song, J., & Ma, J. (2018). Quantification of nitrate sources and fates in rivers in an irrigated agricultural area using environmental isotopes and a Bayesian isotope mixing model. *Chemosphere*, 208, 493–501.
- Zhang, Q. Y., Qian, H., Xu, P. P., Hou, K., & Yang, F. X. (2021). Groundwater quality assessment using a new integrated-weight water quality index (IWQI) and driver analysis in the Jiaokou Irrigation District China. *Ecotoxicology and Environmental Safety*, 212, 12. <https://doi.org/10.1016/j.ecoenv.2021.111992>
- Zhang, J., Chen, L., Hou, X., Ren, X., Li, J., & Chen, Y. (2022a). Hydrogeochemical processes of carboniferous limestone groundwater in the Yangzhuang Coal

- Mine, Huaibei Coalfield. *China. Mine Water and the Environment*, 41(2), 504–517. <https://doi.org/10.1007/s10230-022-00861-y>
- Zhang, J., Chen, L. W., Hou, X. W., Li, J., Ren, X. X., Lin, M. L., . . . Tian, Y. (2022b). Effects of multi-factors on the spatiotemporal variations of deep confined groundwater in coal mining regions, North China. *Science of The Total Environment*, 823, 17. <https://doi.org/10.1016/j.scitotenv.2022.153741>
- Zhong, C. H., Yang, Q. C., Liang, J., & Ma, H. Y. (2022). Fuzzy comprehensive evaluation with AHP and entropy methods and health risk assessment of groundwater in Yinchuan Basin, northwest China. *Environmental Research*, 204, 8. <https://doi.org/10.1016/j.envres.2021.111956>

Publisher's Note Springer Nature remains neutral with regard to jurisdictional claims in published maps and institutional affiliations.

Springer Nature or its licensor (e.g. a society or other partner) holds exclusive rights to this article under a publishing agreement with the author(s) or other rightsholder(s); author self-archiving of the accepted manuscript version of this article is solely governed by the terms of such publishing agreement and applicable law.